

Detection of the Local Structural Changes in the Dimer Interface of *Bam*HI Initiated by DNA Binding and Dissociation Using a Solvatochromic Fluorophore

Koji Nakayama, Masayuki Endo, Mamoru Fujitsuka, and Tetsuro Majima*

The Institute of Scientific and Industrial Research, Osaka University, Mihogaoka 8-1, Ibaraki, Osaka 567-0047, Japan

Received: June 27, 2006; In Final Form: August 10, 2006

To detect the local structural change in an interface between proteins induced by the substrate binding and dissociation, a solvatochromic fluorescent N^{β} -L-alanyl-5-(*N,N*-dimethylamino)-naphthalene-1-sulfonamide (DanAla) was introduced into 132 position of the dimer interface in *Bam*HI. Before addition of the substrate, the fluorescence from the normal planer excited state of DanAla moiety was observed as a main emission, and thereby the DanAla in the dimer interface is located in the hydrophobic microenvironment. The incubation with the substrate for 20 min induced the gradual increase in fluorescence intensity around 430 nm. The fact reflects that the polarity is reduced by the slight structural change initiated by the formation of the complex with the substrate. Furthermore, the incubation for more than 20 min caused the slight decrease in fluorescence around 430 nm and an appearance of fluorescence (560 nm) due to twisted intramolecular charge transfer (TICT) excited state. Therefore, the DanAla is exposed to comparative polar environment after the dissociation of the substrate. The fluorescence lifetime as a minor component, which is attributed to the TICT excited state, was reduced by addition of the substrate. The results provide that the hydrophobicity in the dimer interface is increased by the substrate binding. Interestingly, we found that the structure of an initial form is different from that of a refolded form after the dissociation of the substrate using a spectral subtraction technique. We have achieved detection of the changing structure induced by the substrate binding and dissociation using a steady-state and time-resolved fluorescence.

Introduction

In the past decade, protein–protein interactions are extensively studied in the field of bioscience and medical science.^{1–3} Cellular processes including signal transduction and gene expression are precisely regulated by communications of proteins, and these are finally expressed as biological phenomena such as cell differentiation, cell cycle, and apoptosis. The interfaces between these proteins are generally maintained by hydrogen bonding, electrostatic interaction, and hydrophobic interaction. The chemical and physical properties of the interface between proteins become important factors to determine the binding constant of protein–protein interaction, enzymatic activity, and its affinity. The properties of protein interface are strictly dependent on its structural and environmental conversion, conformational change in polypeptide chain and binding force for protein–protein interaction. However, the properties are easily changed by a trigger such as chemical interaction, substrate binding, pH change, and ion strength change. Thus, it is important to understand how the interfacial change is caused by such stimulus.

Dansyl derivatives are widely used for the characterization of the microenvironment in biomolecules such as DNA,⁴ peptide,^{5,6} and protein^{7–9} because the fluorescence properties are precisely dependent on the polarity of its surrounding. The distinct fluorescence of Dansyl derivatives in polar and nonpolar environments are associated with the emissions from the twisted intramolecular charge transfer (TICT) excited state and the normal planar (NP) excited state, respectively.^{10–12} Upon optical

excitation, although the molecular structure in the NP excited state is similar to that of the ground state, that of the TICT excited state is characterized as twisted structure between dimethylamino and naphthalene moieties. In addition, intramolecular electron transfer in TICT excited state occurs from the dimethylamino group as an electron donor to naphthalene moiety as an electron acceptor, and the full charge separated state is generated. Thus, the properties of the two excited states are quite different. The TICT fluorescence increases in polar environment because the TICT excited state is further charge separated by polar molecules. In contrast, the NP excited state is stable in nonpolar environment because it has no charge separated character. Therefore, the observation of the dual fluorescence from Dansyl derivatives is suitable for the detection of the conversion in microenvironmental polarity. Recent articles introduced detailed studies on protein structural change and difference employing Dansyl moiety modified on a protein.^{13–15} However, there has not been a study on dual fluorescence properties of structural and environmental change in protein interface initiated by a stimulus. In this study, we have tried to pursue interfacial change by repeatable substrate binding and dissociation events using steady-state and time-resolved fluorescence properties from Dansyl moiety.

To investigate the structural change in the interface between proteins using the Dansyl analogue, we employed a restriction enzyme *Bam*HI which exists as a homodimer both in the absence and presence of a substrate DNA (Figure 1A). The salt-bridge networks between specific residues (Lys132, His133, Glu167, and Glu170) allow the formation of the correct dimer, which is required for the expression of the enzymatic activity as shown

* To whom correspondence should be addressed. Phone: (+81)6-6879-8495. Fax: (+81)6-6879-8499. E-mail: majima@sanken.osaka-u.ac.jp.

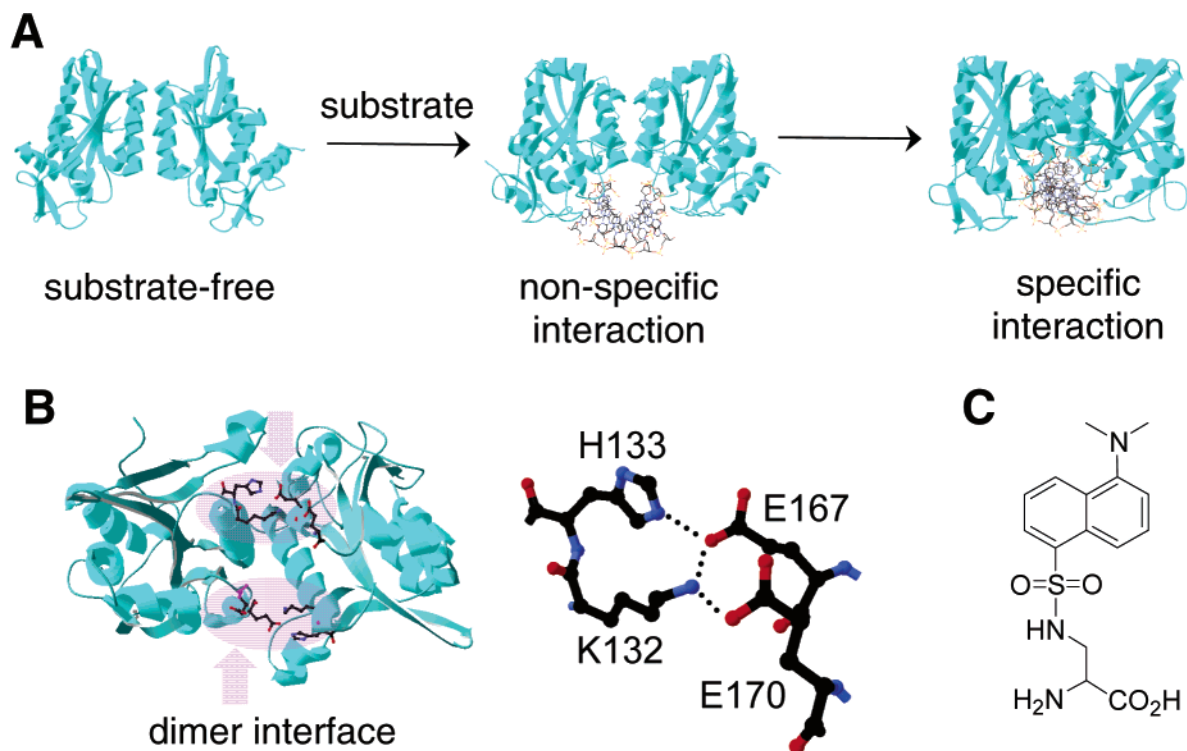


Figure 1. The structure of wild-type *Bam*HI and solvatochromic fluorescent DanAla monomer. (A) Structural change of *Bam*HI dimer induced by the formation of a complex with a substrate DNA. Structures of substrate-free (left), nonspecific interaction with a substrate (middle), and specific interaction with a substrate (right). (B) Crystal structure of *Bam*HI dimer–DNA complex (left). The colored residues represent the key amino acids involved in the formation of the salt-bridge networks in the dimer interface (Lys132, His133, Glu167, and Glu170). Formation of salt-bridge network between side chains of residues in the dimer interface (right). The dashed lines indicate the intermolecular hydrogen bonds in the dimer interface. (C) The structure of solvatochromic fluorescent DanAla monomer.

in Figure 1B.¹⁶ The three distinct *Bam*HI crystal structures were determined as substrate-free and complex with non-specific and specific substrates.¹⁷ However, it has not been reported to monitor the dynamic and real-time structural change induced by the formation of the complex with the substrate using the crystallographic analysis and others.

We planned to monitor the dynamic change of the structure, which is associated with the polarity and viscosity around the Dansyl moiety, with the steady-state and time-resolved spectroscopic measurements. In our previous investigations, we revealed that the introduction of unnatural amino acid into the Lys132 position does not cause the serious misfolding for complete inactivation of the enzyme.^{18–20} Therefore, a solvatochromic fluorescent *N*^β-L-alanyl-5-(*N,N*-dimethylamino)-naphthalene-1-sulfonamide (DanAla) as shown in Figure 1C has been introduced into the 132 position site-specifically using in vitro translation with an expanded codon system.^{21–23} The substrate binding and dissociation events of the mutant (K132Dan), which accompany the slight structural changes, were discriminated using these techniques. In the present work, we discuss the protein motion due to the substrate binding and dissociation events, which were examined using the steady-state and time-resolved spectroscopic measurements of the DanAla moiety in the dimer interface.

Experimental Methods

Materials. Commercially available *Bam*HI was purchased from New England BioLabs (Beverly, MA). L-³⁵S-Methionine was from Amersham Pharmacia Biotech (Piscataway, NJ). T4 RNA ligase was from Takara Shuzo (Kyoto, Japan). T7 RNA polymerase and RNase inhibitor were from Toyobo (Osaka, Japan). RNeasy Mini Kit for RNA purification and a Ni-NTA

spin column were from Qiagen (Hilden, Germany). Micro Bio-Spin 6 Chromatography Column was from Bio-Rad (Hercules, CA). Microcon YM-10 was from Millipore (Billerica, MA). *E. coli* S30 Extract System was from Promega (Madison, WI).

Synthesis of the Mutants Using In Vitro Translation with Expanded Codon System. DanAla-tRNA^{CCCG} was synthesized with the chemical and enzymatic reactions (see description in the Supporting Information available with this article online). The genes for the expression of the wild-type, K132Dan, and H133A/K132Dan mutants were prepared according to our previous report.¹⁸ The preparation of the corresponding mRNA was carried out in solution containing the template DNA (5 μg), T7 RNA polymerase (110 units), NTP (2.5 mM), Tris-HCl (40 mM, pH 7.5), MgCl₂ (20 mM), and DTT (5 mM) at 37 °C for 6 h. The prepared mRNA was purified by spin column of RNeasy Mini Kit. *E. coli* S30 extract system was employed for in vitro translation following the manufacturer's protocol. The in vitro translation for the radioactive assay was carried out in reaction mixture (10 μL) containing mRNA (1 μg), DanAla-tRNA^{CCCG} (1 μg), premix (4 μL), *E. coli* S30 extract (3 μL), amino acid mixture (lacking methionine and arginine) (0.1 mM), arginine (0.01 mM), and ³⁵S-methionine (3 μCi) at 30 °C for 3 h. The wild-type was prepared by the same method without DanAla-tRNA^{CCCG}. The mixtures of proteins were denatured in a solution containing Tris-HCl (50 mM, pH 6.8), DTT (0.1 M), and SDS (2%) and were loaded onto a sodium dodecyl-sulfate polyacrylamide gel electrophoresis (SDS-PAGE) gel (18%). The SDS-PAGE gel was visualized and quantified by an imaging analyzer (Fujix BAS1000 analyzer). On the other hand, to obtain the mutant for the investigation of the fluorescence properties, the large-scale translation was carried out in reaction mixture (100 μL) containing mRNA (10 μg), DanAla-

tRNA^{CCCG} (10 μ g), premix (40 μ L), *E. coli* S30 extract (30 μ L), amino acid mixture (lacking arginine) (1 mM), and arginine (0.1 mM) at 30 °C for 3 h. After the translation, the translation mixtures were diluted in a solution (400 μ L) containing Tris-HCl (10 mM, pH 8.0), MgCl₂ (10 mM), NaCl (300 mM), and imidazole (10 mM), and then the mixtures were loaded onto the Ni-NTA spin columns. The columns bound His-tagged mutants were washed twice by a buffer containing Tris-HCl (10 mM, pH 8.0), MgCl₂ (10 mM), NaCl (300 mM), and imidazole (20 mM). The His-tagged mutants were eluted in a buffer (200 μ L) containing Tris-HCl (10 mM, pH 8.0), MgCl₂ (10 mM), NaCl (300 mM), and imidazole (250 mM). The eluted solution was loaded onto gel filtration spin column (Micro Bio-Spin 6 Chromatography Column, 6 kDa cutoff) in which a buffer was exchanged to Tris-HCl (10 mM, pH 8.0), MgCl₂ (10 mM), NaCl (100 mM), and DTT (1 mM). The excess solution was concentrated up to 100 μ L with Microcon YM-10.

Measurement of the Enzymatic Activity. Enzymatic activities of the wild-type and the mutants were determined by cleavage of pBR322 restriction fragment digested by *Nde*I as the substrate. After the translation at 30 °C for 2 h without the purification, the translation mixtures were diluted by a buffer containing Tris-HCl (10 mM, pH 8.0), MgCl₂ (10 mM), NaCl (100 mM), and DTT (1 mM). The solutions were incubated with the pBR322 restriction fragment at 30 °C for 2 h for checking enzymatic activities. The reaction was stopped by exposure of the sample on ice, and then the mixture was loaded on an agarose gel (1%) containing TBE buffer. The electrophoresis was carried out at 150 V, and then the gel was stained by ethidium bromide. The stained gel was visualized by irradiation of UVB light.

Fluorescence Measurement of the Mutants. After the purification and concentration of K132Dan and H133A/K132Dan mutants using above method, the steady-state and time-resolved fluorescence spectra of the prepared samples were directly measured using a 100- μ L quartz cell (the length of light pass is 1 cm). DanAla moiety in the mutants was excited by irradiation of 320–330-nm light to detect the fluorescence. A short DNA substrate containing the *Bam*HI recognition sequence (5'-CGTGGATCCACG-3': the italics denote the sequence for *Bam*HI recognition) was employed for the detection of the substrate binding and dissociation events. The steady-state fluorescence was measured at room temperature using a Hitachi 850 Fluorescence Spectrometer. The time-resolved fluorescence was measured at <15 °C to avoid the enzymatic digestion of the substrate during this experiment. The fluorescence lifetime in the sub-picosecond to nanosecond time region was performed by the single-photon counting method using the second harmonic generation (SHG, 430 nm) of a Ti-sapphire laser (Spectra-Physics, Tsunami 3941-M1BB, fwhm 100 fs) as the excitation source. Fluorescence from the DanAla analogues was detected using a streak camera (Hamamatsu Photonics (4354)) equipped with a polychromator (Acton Research Spectra Pro 150). The lifetimes of the K132Dan and H133A/K132Dan mutants were measured in the absence and presence of cofactor Mg²⁺ (10 mM) and excess substrate DNA.

Results

Site-Selective Incorporation of DanAla into Lys132 Position of *Bam*HI. The wild-type and the mutants were expressed by *E. coli* S30 cell free translation system with radioactive ³⁵S-methionine containing the corresponding mRNAs in the absence and presence of DanAla-tRNA^{CCCG}, respectively. The translation mixtures were loaded onto a SDS-PAGE gel, and then the

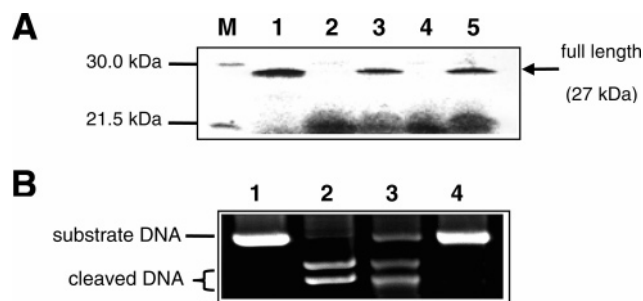


Figure 2. Protein synthesis and enzymatic activity of the wild-type *Bam*HI and K132Dan and H133A/K132Dan mutants. (A) SDS-PAGE of translation products of the wild-type *Bam*HI and the mutants. Translation products with wild-type mRNA (lane 1), mutated mRNA without and with DanAla-tRNA^{CCCG} (lanes 2 and 3, respectively), translation products with mutated mRNA (H133A) without and with DanAla-tRNA^{CCCG} (lanes 4 and 5, respectively), lane M, molecular weight marker (21.5 and 30.0 kDa). (B) Cleavage of the substrate (pBR322 restriction fragment digested by *Nde*I) with wild-type *Bam*HI and the mutants. Substrate only (lane 1), digestion of the substrate with wild-type (lane 2), K132Dan mutant (lane 3), and H133A/K132Dan mutant (lane 4).

radioactive products in the gel were visualized by an imaging analyzer (Figure 2A). The wild-type was expressed as a full-length protein of which molecular weight is approximately 27 kDa (lane 1). As a control experiment, the translations of K132Dan and H133A/K132Dan mutants were performed in the absence of DanAla-tRNA^{CCCG} in the translation mixture, so that truncated bands appeared at approximately 20 kDa (lanes 2 and 4, respectively). In contrast, the expressions of two mutants were performed in the presence of DanAla-tRNA^{CCCG}, which resulted in the full-length bands of K132Dan and H133A/K132Dan mutants as well as the wild-type (lanes 3 and 5, respectively). These results indicate that DanAla-tRNA^{CCCG} specifically recognizes the CGGG four-base codon in the mutated mRNA and that DanAla is introduced into the 132 position of the protein site-specifically. In contrast, the truncated peptides having low molecular weight around 20 kDa are expressed when the three-base anti-codon in the inherent Arg-tRNA^{CCG} recognizes the CGG three-base in the four-base codon (CGGG) of the mutated mRNA. The incorporation efficiencies of K132Dan and H133A/K132Dan mutants were 21 and 18%, respectively. Therefore, the recognition of Arg-tRNA^{CCG} as CGG codon is occurred rather than that of DanAla-tRNA^{CCCG} as CGGG codon preferentially. In the previous report, the incorporation efficiency of 1-naphthylalanine at Tyr83 of streptavidin is 30%, indicating that the 1-naphthylalanine represents higher incorporation efficiency than DanAla because the smaller 1-naphthylalanine is easier to be accepted by *E. coli* ribosome than relatively bulky DanAla.²²

Enzymatic Activities of the K132Dan and H133A/K132Dan Mutants. The activity of the wild-type and the two mutants was estimated by the cleavage of a substrate DNA employing a linear pBR322 digested by *Nde*I (Figure 2B). Although the molecular weight of the substrate is 4361 bp, the 1920- and 2441-bp fragments of the cleaved substrate should be generated by precise *Bam*HI enzymatic activity. Commercially available wild-type *Bam*HI showed the sufficient activity and sequence selectivity (lane 2). K132Dan mutant represented the sequence selective digestion because the correct fragments appeared in the gel (lane 3). The site-specific digestion of the substrate suggests that the formation of the correct dimer to express the enzymatic activity is not inhibited by the introduced DanAla. However, the efficiency of the activity was slightly reduced compared to the wild-type. On the other hand,

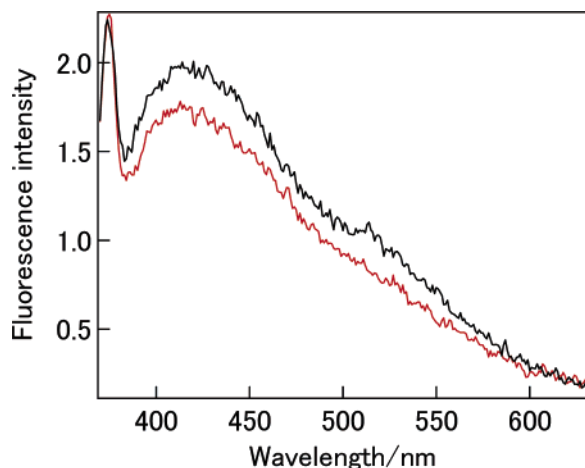


Figure 3. The normalized steady-state fluorescence spectra of K132Dan (black) and H133A/K132Dan (red) mutants. The DanAla moiety in these mutants was excited at 330 nm. The sharp peak at 374 nm is ascribed to Raman scattering.

the intrinsic activity of the H133A/K132Dan mutant was significantly reduced by mutation of H133 in K132Dan mutant (lane 4). The inactivation indicates that the dual mutation to remove the salt-bridge networks between the monomers causes the significant inhibition of the active dimerization.

Steady-State Fluorescence of K132Dan and H133A/K132Dan Mutants. The steady-state fluorescence of K132Dan and H133A/K132Dan mutants were measured before addition of the substrate (Figure 3). The sharp peak at 374 nm is ascribed to the Raman spectrum. The broad fluorescence spectra of K132Dan and H133A/K132Dan mutants were observed, and the fluorescence maxima appeared at 423 and 413 nm, respectively. On the other hand, the fluorescence maximum of DanAla monomer in *n*-hexane was observed at 460 nm (see fluorescence spectra of DanAla monomer in the Supporting Information (Figure 1S) available with this article online), and the characteristic fluorescence is ascribed to the emission from the TICT excited state.¹² The fluorescence maxima of these mutants represent significant blue-shift as compared to that of DanAla monomer in hydrophobic *n*-hexane. In a previous report, the maximum of the fluorescence from the NP excited state (b^* band) in nonpolar benzene is observed at around 400 nm.¹² Therefore, the fluorescence spectra obtained from two mutants should be ascribed to emission from the NP excited state as a major component. We revealed that the micropolarity around the DanAla at the 132 position shows the strong hydrophobic property. On the other hand, the fluorescence maximum of H133A/K132Dan was located at a shorter wavelength than that of K132Dan mutant. The experimental result strongly suggests that the DanAla in H133A/K132Dan mutant is located in a more hydrophobic site as compared to that in K132Dan mutant.

In a different perspective, we discuss the hydrophobicity in the dimer interface of these mutants by analyzing the emission from the TICT excited state which is more stable in a hydrophilic environment. The steady-state fluorescence spectrum of the K132Dan mutant has a shoulder around 514 nm, which is ascribed to the generation of TICT excited state as a minor component. On the other hand, the TICT emission of H133A/K132Dan mutant is not clearly observed. The result supports that the hydrophobicity in the dimer interface of the K132Dan mutant is stronger than that of the H133A/K132Dan mutant.

The minimized structure around the dimer interface in the K132Dan mutant was estimated to obtain evidence that the microenvironment shows hydrophobic property. As a result of

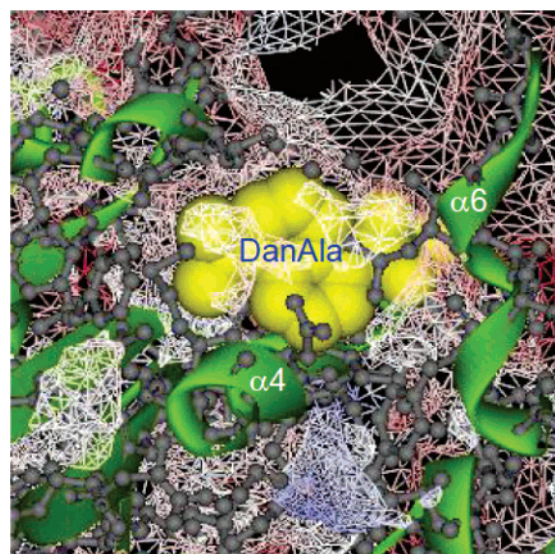


Figure 4. The dimer interface in the minimized structure of the K132Dan mutant. The yellow colored molecule denotes the DanAla moiety introduced into the 132 position. The three-dimensional mesh shows the outer surface of the mutant; the red- and blue-colored areas represent negative and positive potentials, respectively. The white area shows the hydrophobic surface. The green colored loop denotes α -helices in the mutant. The minimization of the structure was carried out using a DS Viewer Pro software.

the estimation, we found that the DanAla moiety is located in the hydrophobic space (Figure 4). Additionally, the simulated structure reveals that the DanAla moiety is trapped in the rigid polypeptide chain. The estimation of the local structure strongly supports the results of the steady-state fluorescence spectroscopic measurement.

Time-Resolved Fluorescence of K132Dan and H133A/K132Dan Mutants. Type II restriction endonuclease including *Bam*HI requires Mg^{2+} as a cofactor to catalyze the hydrolysis reaction of the DNA phosphodiester backbone. According to a previous report, the structure in wild-type *Bam*HI is identified as three distinct structures (substrate-free, specific interaction with substrate, and nonspecific interaction with nonsubstrate DNA).¹⁷ To obtain additional information about the environments of the dimer interface in the distinct structural mutants, we measured the fluorescence lifetimes in the K132Dan and H133A/K132Dan mutants with the method of femtosecond time-resolved fluorescence spectroscopic measurement. In the present experiment, the temperature for the measurement of the time-resolved fluorescence was kept at $<15^\circ\text{C}$ to avoid the enzymatic digestion of the substrate during the experiment. The lifetimes of the K132Dan and H133A/K132Dan mutants were measured in the absence and presence of cofactor Mg^{2+} and substrate DNA (Table 1).

In the case of the K132Dan mutant, we found that the lifetimes were estimated as distinct values in the absence and presence of the substrate. The difference of the lifetimes between the two mutants reflects the structural transition induced by the formation of the complex with the substrate. Furthermore, we found that the binding of the cofactor Mg^{2+} does not affect the lifetime in this experiment, which indicates that the structural change in the dimer interface is not induced by the formation of a complex (protein- Mg^{2+} -DNA) in the active site.²⁴ On the other hand, the lifetime of H133A/K132Dan mutant was not changed by addition of the substrate and the cofactor. The result suggests that the H133A/K132Dan mutant has no ability to bind the substrate because of the suppression of the salt-bridge network in the dimer interface. Therefore, the structure

TABLE 1: Fluorescence Lifetimes (τ_f) of K132Dan and H133A/K132Dan Mutants in the Absence and Presence of Substrate DNA and Cofactor Mg^{2+}

BamHI mutant	substrate DNA ^a	cofactor Mg^{2+} ^a	τ_f (ns)
K132Dan	—	—	1.7 (86%), 10.8 (14%)
K132Dan	+	—	1.3 (82%), 7.6 (18%)
K132Dan	+	+	1.1 (83%), 7.4 (17%)
H133A/K132Dan	—	—	2.4 (69%), 11.7 (31%)
H133A/K132Dan	+	—	2.0 (74%), 11.3 (26%)
H133A/K132Dan	+	+	1.9 (73%), 11.4 (27%)

^a Minus and plus mean the absence and presence of substrate DNA and cofactor Mg^{2+} , respectively. The fluorescence decays were analyzed by two components with the ratios in %.

in the H133A/K132Dan mutant is not changed the structure such as the K132Dan mutant when the substrate is added. The structure of the H133A/K132Dan is no longer similar to that of K132Dan mutant as well as the wild-type, and the suppression of the salt-bridge networks in the dimer interface leads to the inhibition of the correct protein–protein interaction to bind the substrate.

The fluorescence decays of the two mutants showed distinct multiexponential curves. The several components with distinct lifetimes are due to the varied anisotropy of the fluorophore, which is located in the rigid polypeptide matrix. Zewail and co-workers described that a decay component of the Dan derivative observed at 430 nm has a lifetime of ~ 900 ps and is ascribed to a relaxation from the locally excited state after solvation and below the twisting barrier.²⁵ Since the fluorescence peak and lifetime are similar to those in the present study, we can interpret that the main component of the two mutants which has a short lifetime (~ 2 ns) is due to faster radiative relaxation from the NP excited state of the DanAla moiety after the solvation. The minor component having a longer lifetime (7–12 ns) is attributed to radiative relaxation from the TICT excited state, which is generated from the NP excited state. In the case of K132Dan, the lifetime of the minor component was reduced when the substrate was added. It is well known that the fluorescence lifetime of the TICT excited state is reduced when a Dan derivative is located in a hydrophobic environment.^{26,27} Therefore, the decrease in the fluorescence lifetime induced by addition of the substrate suggests that the hydrophobicity is increased by local structural change caused by the formation of the complex.

Structural Change in K132Dan Mutant Initiated by Formation of the Complex with the Substrate. To monitor the structural change initiated by the formation of the complex with the substrate and the following digestion, we tried to measure steady-state fluorescence spectral conversion of K132Dan mutant caused by the incubation with the excess substrate at 37 °C. The spectral conversion upon the incubation time for the formation of the complex and the following digestion is presented in Figure 5A. As described in the prevent result, the fluorescence at 430 nm is attributed to the emission from the NP excited state in the absence of the substrate, indicating that the dimer interface shows hydrophobic environment. After the addition of the excess substrate, the fluorescence intensity was gradually increased upon the incubation time up to ~ 20 min. However, the incubation for more than 20 min caused the gradual decrease in fluorescence intensity, and also the fluorescence shoulder in the longer wavelength region (longer than 500 nm) appeared in 30 min. Although the incubation for more than 40 min was carried out, no more spectral change was observed. It is thought that this fluorescence behavior to ~ 20 min is due to the structural motion of the dimer interface induced

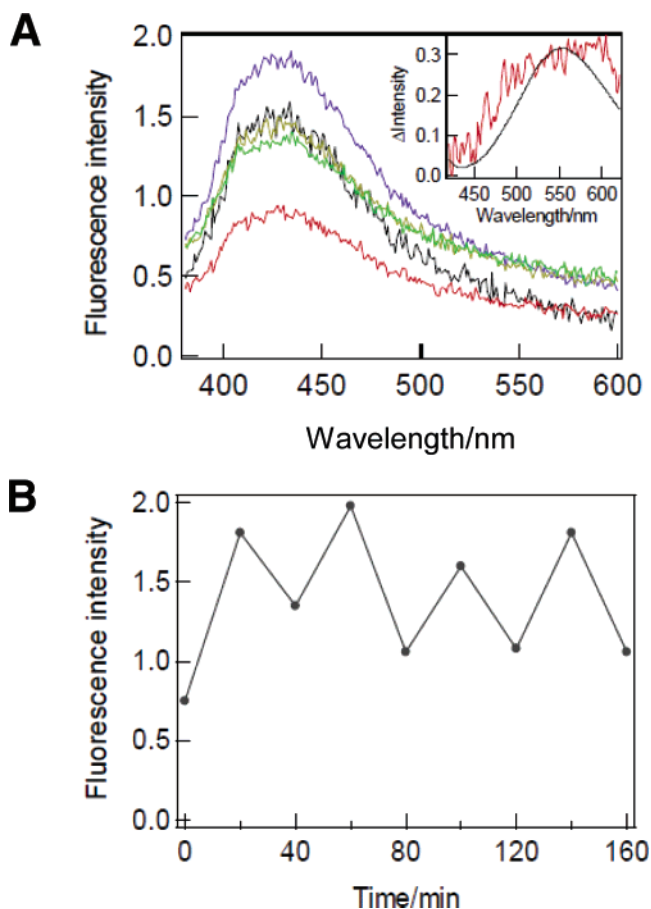


Figure 5. Time-dependent fluorescence spectra and intensity of K132Dan mutant in several incubation times. The mutant was irradiated at 320 nm to detect the fluorescence change. (A) The fluorescence spectra of K132Dan mutant with the substrate in different incubation times for 2 (red), 10 (black), 20 (blue), 30 (yellow), and 40 min (green), respectively. Inset: differential spectrum between the fluorescence spectra in 0 and 40 min (red) and fluorescence spectrum of DanAla monomer in Tris-HCl buffer (pH 8.0) (black). (B) The fluorescence intensity of repeatable substrate binding and dissociation. The relative fluorescence intensity at 430 nm is plotted at every 20-min incubations. The excess substrate was added to the K132Dan mutant mixture, and then the fluorescence was measured every 20 min during the incubation. After the incubation for every 40 min, the same amount of the substrate was added again and the fluorescence was measured every 20 min.

by gradual formation of the complex with the substrate. The slow binding of the substrate may be caused by the significant decrease of the activity of the K132Dan mutant as compared to that of the wild-type (Figure 2B).

The differential spectrum between initial (0 min) and final (40 min) spectra is shown in the inset of Figure 5A (red). As a referential experiment, the fluorescence spectrum of DanAla monomer was measured in Tris-HCl buffer before the introduction of the fluorophore into the specific position (see fluorescence spectra of DanAla monomer in the Supporting Information (Figure 1S) available with this article online). The differential spectrum is in agreement with the spectrum of DanAla monomer in Tris-HCl buffer (black). This result indicates that the TICT excited state is generated after dissociation of the substrate, and the hydrophobicity in the dimer interface is reduced by the dissociation of the substrate. Furthermore, the structure of K132Dan mutant before substrate binding is slightly different from that after substrate dissociation.

To investigate the reproducibility of the structural change, we monitored the change of the fluorescence intensity using real time steady-state fluorescence during the binding of the

substrate and the following dissociation of the cleaved substrate (Figure 5B). The fluorescence intensity at 430 nm was monitored and plotted every 20 min (prior to incubation without the substrate (0 min) and the following incubation with the excess substrate for 20 and 40 min). As described above, the increase and decrease in the intensity in the 20 and 40 min incubation suggests the local structural change induced by the substrate binding to the mutant and the dissociation from the mutant, respectively. Furthermore, the addition of the same amount of the substrate and then following substrate and incubation for more 20 and 40 min (total incubation time in Figure 5B, 60 and 80 min, respectively) were carried out. The fluorescence conversion of at least four cycles was repeated by local structural change in the dimer interface induced by substrate binding and dissociation events.

Discussion

We have demonstrated that the local structure in *Bam*HI is gradually changed by binding and dissociation of a substrate DNA using steady-state and time-resolved fluorescence properties by the excited DanAla moiety, which is introduced into the 132 position site-specifically. This method plays an important role to monitor local structural change as well as slight environmental change even though the concentration of a protein is much low.

The enzymatic activity of the two mutants provides important information on the protein structure. In the present study, the specific digestion of the substrate using K132Dan mutant suggests that the DanAla introduced in the K132 position exhibits the formation of the correct dimer to express the enzymatic activity similar to wild-type *Bam*HI, but the intrinsic enzymatic activity was slightly reduced by the introduction of DanAla moiety (lane 3 in Figure 2B). The similar phenomenon was observed when *cis*-phenylazophenylalanine derivatives were introduced into the same position of *Bam*HI, in which the V_{\max} value decreased by one order of magnitude as compared to that of the wild-type.²⁰ Therefore, we revealed that the introduction of an unnatural amino acid into the 132 position results in the decrease in the enzymatic activity caused by the reduction of the V_{\max} value. On the other hand, H133A/K132Dan mutant showed the significant inhibition of the intrinsic activity (lane 4 in Figure 2B). The dual mutation to remove the salt-bridge networks between the monomers causes the inhibition of the active dimerization. In our recent investigation, the similar inhibition of the enzymatic activity was observed when we have investigated the enzymatic activity of another photofunctionalized *Bam*HI (H133A/ K132K^{NVOC}), which was mutated by the introduction of photoeliminative 6-nitroveratryloxycarbonyl (NVOC) group into the ϵ -amino group of Lys132 residue in H133A mutant.¹⁸ However, after the introduced NVOC group was eliminated by photoirradiation at 366 nm for 20 min, the resulting mutant expressed the activity. This result implies that the salt-bridge network in the mutant is precisely formed between the residues (Lys132, Glu167, and Glu170) after the removal of NVOC group. In the above report, we have tried to detect the dimer and monomer structures of H133A/K132K^{NVOC} mutant by investigation of a chemical cross-linking reaction. The result represented that the inhibition of salt-bridge network formation in the dimer interface did not affect the dimerization but strongly caused the inactivation. Therefore, the structure of H133A/K132K^{NVOC} mutant is considered as an inactive dimer. The previous experimental evidence supports that inactive H133A/K132Dan mutant allows the formation of the dimer structure, which differs from wild-type *Bam*HI and active

K132Dan mutant. Although the binding affinity between H133A/K132Dan monomers still remains, the ability of the specific protein–protein interaction is abolished by the mutation for the suppression of the salt-bridge network formation. The difference in the local structure of the dimer interface represents the distinction in peak position and TICT emission intensity in the spectrum. In the case of K132Dan mutant, it can therefore be indicated that the salt-bridge network between His133 and Glu167 is not interrupted by the introduced DanAla because the DanAla is located on the opposite site of the salt-bridge network. This interpretation supports the fact that the mutant has the precise salt-bridge network, which requires expressing the correct enzymatic activity as shown in the investigation of the enzymatic activity. On the other hand, the H133A/K132Dan mutant should form dimer structure through only hydrophobic interaction because the substituted Ala133 residue is not allowed to form the salt-bridge network with the Glu167 residue in the counterpart helix. In addition, the polarity is low enough not to generate the TICT excited state, which is stabilized by reorientation of water molecules, suggesting that water molecules are excluded from the site around the DanAla at the 132 position. The shoulder in the fluorescence spectrum of the K132Dan mutant provides the information on the generation of the TICT excited state, indicating that the environment of the dimer interface of K132Dan mutant is relatively hydrophilic as compared to that of the H133A/K132Dan mutant.

There are reports focused on fluorescence probes, which monitor not only the polarity but also the rigidity of medium.^{27–29} According to a description proposed by Neckers et al., medium viscosity strongly influences its mobility of the medium to stabilize the polar TICT excited state relaxed from locally excited state (NP excited state) of which structure is similar to that of its ground state.^{30,31} Therefore, the fluorescence peaks of the mutants which were observed at shorter wavelength side compared with the fluorophore monomer are dependent on the rigidity as well as the polarity. After the vibrational relaxation from the Franck–Condon state, the mobility and reorientation of the flexible medium to stabilize the polar TICT excited state easily occurred within the lifetime of the NP excited state, and thereby the fluorescence from the TICT excited state is observed.³² On the other hand, the increase in microviscosity inhibits the relaxation of the NP excited state to its lowest TICT excited state because the reorientation of the viscous medium does not occur within the lifetime of the NP excited state. In the present investigation, the environment of the inner protein, which is quite rigid and complex, is regarded as a viscous matrix consisting of rigid polypeptide network. This description means that the mobility and reorientation of the polypeptide chain to stabilize the polar TICT excited state of the DanAla moiety are negligible, and thereby the main fluorescence of the two mutants is due to the emission from locally excited state (NP excited state). Furthermore, the fluorescence maximum of the H133A/ K132Dan mutant appeared in shorter wavelength than that of K132Dan mutant. This phenomenon provides the possibility that the DanAla moiety in the H133A/K132Dan mutant may be buried in the rigid hydrophobic polypeptide chain by the local misfolding; however the K132Dan mutant would be located in the normal environment like a flexible space on the interface. Thus, the DanAla residue is an important probe for the estimation of the viscosity and rigidity of a polypeptide chain in a protein as well as the polarity due to a microstructure.

The lifetimes of the fluorescence also provide information about the polarity in a protein microenvironment. The main component having a lifetime of ~ 2 ns is ascribed to faster

radiative relaxation from the NP excited state. In contrast, the minor component having a lifetime of more than 10 ns is ascribed to relaxation from the TICT excited state.³³ According to some reports, it has been proposed that the fluorescence from Dan group is strongly quenched in a hydrophilic environment.^{26,34} In this study, the lifetime of DanAla in the K132Dan mutant became shorter when the substrate was added. This phenomenon indicates that the peptide chain gradually moves to form the precise complex with the substrate, and finally the environment in the dimer interface is converted to the higher polarity as compared to that of the substrate-free mutant. After the digestion of the substrate, the cleaved substrates are dissociated from the active site, and then the refolding to initial structure is initiated to bind the substrate again. As a result of differential spectrum, we have revealed the formation of TICT excited state after the dissociation. Interestingly, the interface environment refolded from the substrate binding form represents slightly higher polarity as compared to that of the initial form which is prior to substrate binding event. An accessible space of water molecules might appear in the dimer interface because rigid polypeptide chain is relaxed by refolding to substrate-free form. The repeatable fluorescence change was observed by the substrate binding and dissociation events, and thereby the mutant had ability to repeat binding and digestion of the substrate. The lifetime of H133A/K132Dan mutant was longer than that of K132Dan mutant. This result is probably associated with the effect of the hydrophobic Ala133 residue. In the above discussion, we have revealed that H133A/K132Dan mutant represents inactivation caused by serious misfolding. The fact provides an explanation as to why the $\alpha 4$ helix containing DanAla and Ala133 residues no longer forms native helical structure, and DanAla moiety would be buried in hydrophobic site of the rigid polypeptide matrix.

The time dependence of steady-state fluorescence upon addition of substrate DNA to the K132DanAla mutant is interpreted as resulting from time-dependent binding of the substrate and time-dependent release of cleaved substrates. The real-time spectral change upon addition of the substrate reflects rapid saturation of the substrate in DNA-binding site, which may be faster than the substrate cleavage reaction, up to 20 min. The cleavage of the substrate and following release of cleaved substrates occurred as a main behavior of the enzyme from 20 to 40 min. The final structure (after enzymatic reaction finished) was clearly different from the initial one (before the reaction) because the final structure had an ability to generate a TICT excited state. The final structure allowed the binding of new substrate until the substrate was depleted because the fluorescence increased upon addition of the substrate. In the viewpoint of the enzymatic reaction rate, we previously determined the substrate affinity and rate of enzymatic reaction using a similar mutant which had a nonnatural amino acid in K132 position.^{18,20} As a result, both of the parameters of the mutants were reduced by the mutation compared to those of wild-type *Bam*HI. In the present investigation, the ability to cleave the substrate should be decreased by introduction of DanAla in the same position, suggesting that the rate may be not as large as that of wild-type.

Conclusions

We have characterized the fluorescence behavior of the DanAla incorporated in the interface of *Bam*HI using its solvatochromic property. From the steady-state fluorescence spectroscopic measurement, we estimated the hydrophobicity and viscosity of the environment in the dimer interface of

*Bam*HI. The complex formation of K132Dan mutant with substrate DNA has been directly monitored, and the differences in the spectral shapes and fluorescence lifetimes of the DanAla moiety between the substrate-free and substrate-bound *Bam*HI reflect the local structural change in the dimer interface. Fluorescence lifetimes can discriminate distinct states of the *Bam*HI dimers such as substrate-free and substrate-bound forms, which are the very slight structural changes. The repeated motions of the substrate binding and dissociation events can be also observed with the steady-state fluorescence spectroscopic measurement. The substrate-induced structural change of the dimer interface can be consecutively monitored by tracing the fluorescence of the DanAla moiety. Importantly, these motions can be detected in the dimer interface, which is located in the different side of the substrate-binding site. This finding suggests that the dimer interface may move slightly as a hinge when the *Bam*HI dimer captures and releases the substrate. We have demonstrated that the site selectively introduced DanAla is a powerful tool for the detailed detection of the local structural change and the estimation of the microenvironment change in the movable protein–protein interface.

Acknowledgment. This work has been partly supported by a Grant-in-Aid for Scientific Research (Project 17105005, Priority Area (417), 21st Century COE Research, and others) from the Ministry of Education, Culture, Sports, Science and Technology (MEXT) of Japanese Government.

Supporting Information Available: The organic synthesis of DanAla derivatives, the ligation of DanAla to tRNA^{CCCC}, and the fluorescence spectra of DanAla monomer and DanAla-tRNA^{CCCC}. This material is available free of charge via the Internet at <http://pubs.acs.org>.

References and Notes

- (1) Zhang, Y.; Takami, K.; Lo, M. S.; Huang, G. M.; Yu, Q.; Roswit, W. T.; Holtzman, M. J. *J. Biol. Chem.* **2005**, *280*, 34306.
- (2) Rousseau, F.; Schymkowitz, J. *Curr. Opin. Struct. Biol.* **2005**, *15*, 23.
- (3) Rhodes, D. R.; Tomlins, S. A.; Varambally, S.; Mahavisno, V.; Barrette, T.; Kalyana-Sundaram, S.; Ghosh, D.; Pandey, A.; Chinnaiyan, A. M. *Nature Biotechnol.* **2005**, *23*, 951.
- (4) Jadhav, V. R.; Barawkar, D. A.; Ganesh, K. N. *J. Phys. Chem.* **1999**, *103*, 7383.
- (5) Kuribayashi, H.; Takahashi, T.; Nagata, K.; Ueno, A.; Mihara, H. *Bioorg. Med. Chem. Lett.* **2000**, *10*, 2227.
- (6) Wang, R.; Bright, F. V. *J. Phys. Chem.* **1993**, *97*, 10872.
- (7) Enander, K.; Dolphin, G. T.; Liedberg, B.; Lundström, I.; Baltzer, L. *Chem.—Eur. J.* **2004**, *10*, 2375.
- (8) Cohen, B. E.; McAnaney, T. B.; Park, E. S.; Jan, Y. N.; Boxer, S. G.; Jan, L. Y. *Science* **2002**, *296*, 1700.
- (9) Pal, S. K.; Zewail, A. H. *Chem. Rev.* **2004**, *104*, 2099.
- (10) Wang, Z. J.; Song, J. C.; Bao, R.; Neckers, D. C. *J. Polym. Sci. B* **1996**, *34*, 325.
- (11) Parusel, A. B. J.; Nowak, W.; Grimme, S.; Köhler, G. *J. Phys. Chem. A* **1998**, *102*, 7149.
- (12) Ren, B. Y.; Gao, F.; Tong, Z.; Yan, Y. *Chem. Phys. Lett.* **1999**, *307*, 55.
- (13) Williams, E. C.; Janmey, P. A.; Ferry, J. D.; Deane, F. M. *J. Biol. Chem.* **1982**, *257*, 14973.
- (14) Bekos, E. J.; Ranieri, J. P.; Aebischer, P.; Gardella, J. A., Jr.; Bright, F. V. *Langmuir* **1995**, *11*, 984.
- (15) Backovic, M.; Stratikos, E.; Lawrence, D. A.; Gettins, P. G. W. *Protein Sci.* **2002**, *11*, 1182.
- (16) Newman, M.; Strezlecka, T.; Dorner, L. F.; Schildkraut, I.; Aggarwal, A. K. *Structure* **1994**, *2*, 439.
- (17) Viadiu, H.; Aggarwal, A. K. *Mol. Cell* **2000**, *5*, 889.
- (18) Endo, M.; Nakayama, K.; Majima, T. *J. Org. Chem.* **2004**, *69*, 4292.
- (19) Nakayama, K.; Endo, M.; Majima, T. *Chem. Commun.* **2004**, *21*, 2386.
- (20) Nakayama, K.; Endo, M.; Majima, T. *Bioconj. Chem.* **2005**, *16*, 1360.

- (21) Hohsaka, T.; Ashizuka, Y.; Murakami, H.; Sisido, M. *J. Am. Chem. Soc.* **1996**, *118*, 9778.
- (22) Hohsaka, T.; Kajihara, D.; Ashizuka, Y.; Murakami, H.; Sisido, M. *J. Am. Chem. Soc.* **1999**, *121*, 34.
- (23) Endo, M.; Nakayama, K.; Kaida, Y.; Majima, T. *Angew. Chem., Int. Ed. Eng.* **2004**, *43*, 5643.
- (24) Viadiu, H.; Aggarwal, A. K. *Nature Struct. Biol.* **1998**, *5*, 910.
- (25) Zhong, D.; Pal, S. K.; Zewail, A. H. *ChemPhysChem* **2001**, *2*, 219.
- (26) Leick, V. *J. Cell Sci.* **1992**, *103*, 565.
- (27) Popielarz, R.; Hu, S. K.; Neckers, D. C. *J. Photochem. Photobiol. A* **1997**, *110*, 79.
- (28) Loutfy, R. O. *Macromolecules* **1981**, *14*, 270.
- (29) Loutfy, R. O.; Teegarden, D. M. *Macromolecules* **1983**, *16*, 452.
- (30) Paczkowski, J.; Neckers, D. C. *Macromolecules* **1991**, *24*, 3013.
- (31) Song, J. C.; Neckers, D. C. *Polym. Eng. Sci.* **1996**, *36*, 394.
- (32) Jager, W. F.; Volkers, A. A.; Neckers, D. C. *Macromolecules* **1995**, *28*, 8153.
- (33) Banik, U. B.; Mandal, N. C.; Bhattacharyya, B.; Roy, S. *J. Biol. Chem.* **1993**, *25*, 3938.
- (34) Huang, S.; Klingenberg, M. *Biochemistry* **1995**, *34*, 349.